ELSEVIER

Global and Planetary Change 32 (2002) 89–109

GLOBAL AND PLANETARY CHANGE

www.elsevier.com/locate/gloplacha

On modelling present-day and last glacial maximum oceanic $\delta^{18}O$ distributions

Martin R. Wadley [a,*], Grant R. Bigg [a], Eelco J. Rohling [b], Antony J. Payne [c]

[a] School of Environmental Sciences, University of East Anglia, Norwich, UK
[b] School of Ocean and Earth Sciences, Southampton Oceanography Centre, University of Southampton, European Way, Southampton, SO14 3ZH, UK
[c] Department of Geography, University of Southampton, Highfield, Southampton, SO17 1BJ, UK

Received 20 April 2000; received in revised form 27 December 2000; accepted 8 January 2001

Abstract

Present-day (PD) and Last Glacial Maximum (LGM) simulations of the global ocean are presented, with the oxygen-18 isotope included as a passive tracer. The gradient of the PD North Atlantic surface $\delta^{18}O$:salinity relationship is found to result from different processes at low and high latitudes. At low latitudes, the balance between surface ^{18}O flux and oceanic advection and mixing sets the surface $\delta^{18}O$:salinity gradient, whereas at high latitudes, mixing between ^{18}O-depleted runoff and precipitation to the Arctic, Bering Strait inflow, and waters from lower latitudes, controls the $\delta^{18}O$:salinity gradient. The importance of the Bering Strait contribution has not previously been recognised. These gradients change significantly at the LGM, and are found to be sensitive to both Arctic runoff $\delta^{18}O$ concentrations and changes in oceanic advection, particularly the rate of exchange of North Atlantic deep water with the global ocean. It is concluded that reconstructions of past climates from records of sea surface $\delta^{18}O$ based on analogues of the PD $\delta^{18}O$:salinity relationship are likely to be in error. © 2002 Elsevier Science B.V. All rights reserved.

Keywords: oxygen isotopes; ocean model; North Atlantic; Last Glacial Maximum

1. Introduction

The ratio of $^{18}O/^{16}O$ isotopes in seawater can be used to help understand the circulation of the ocean, both for the present (e.g. Östlund and Hut, 1984; Ferronsky and Brezgunov, 1982; Bauch et al., 1995; Frew et al., 1995; Gat et al., 1996) and in the past (e.g. Labeyrie et al., 1987; Shackleton, 1987; Duplessy et al., 1993; Wang et al., 1995). In Vienna standard mean ocean water (VSMOW), the atomic ratio of $^{18}O/^{16}O$ is $[2005.20 \pm 0.45] \times 10^{-6}$ (Baertschi, 1976), but it is more commonly measured in ‰ such that:

$$\delta^{18}O = \frac{[(^{18}O/^{16}O)_{sample} - (^{18}O/^{16}O)_{VSMOW}]}{(^{18}O/^{16}O)_{VSMOW}} \times 1000‰. \quad (1)$$

Fluxes of fresh water to and from the ocean bring with them an isotopic signature which depends on the processes governing the fresh water flux. Water molecules containing the ^{16}O isotope are preferentially

* Corresponding author. Tel.: +44-1603-456161; fax: +44-1603-507719.
E-mail address: m.wadley@uea.ac.uk (M.R. Wadley).

0921-8181/02/$ - see front matter
PII: S0921-8181(01)00084-4

evaporated, leaving the ocean enriched in ^{18}O. Condensation of water vapour in the atmosphere leading to precipitation preferentially removes $H_2{}^{18}O$ from the atmosphere. This means that surface waters of the ocean are enriched in ^{18}O at low latitudes, and depleted at high latitudes (Gat, 1996). The precipitation, evaporation and runoff flux to the ocean also changes the salinity. The changes in $\delta^{18}O$ in surface ocean waters, however, depend on both the amount of fresh water added, and its $\delta^{18}O$ content. The $\delta^{18}O$ signature is transported by advective and diffusive processes in the ocean, so that an equilibrium balance is achieved. The relationship between salinity and $\delta^{18}O$ in the ocean, therefore, results from both the spatial variation of $\delta^{18}O$ associated with the fresh water flux to the ocean and the nature of the oceanic circulation (Rohling and Bigg, 1998).

The $\delta^{18}O$ record contained in deep-sea cores has provided much of the evidence for long-term variability in the oceans. Provided local temperature variations are assumed to be small, or can be constrained by other methods such as faunal assemblages or alkenone ratios, a residual record of variations in background ratio can be derived. For benthic $\delta^{18}O$, the ratio has been interpreted as a global ice-volume record (e.g. Shackleton, 1987). Palaeosalinity has been derived from planktonic foraminifera (e.g. Duplessy et al., 1993), assuming that the linear relationship between $\delta^{18}O$ and salinity in the present-day ocean is unchanged from the past. However, there is now evidence that the $\delta^{18}O$:salinity relationship is likely to have changed through time. In particular, changes in the oceanic advection and fresh water budgets of $\delta^{18}O$ could vary the $\delta^{18}O$:sa-O:salinity relationship (Rohling and Bigg, 1998). The $\delta^{18}O$:salinity relationship has also been found to change with time in an ocean simulation, in response to adjustment of the modelled ocean circulation to surface forcing (Schmidt, 1998).

In this paper, we use recent advances in ocean modelling, including an efficient ocean general circulation model (OGCM) with a curvilinear grid and variable time stepping (Wadley and Bigg, 2000, 2001), in conjunction with the experience gained from previous $\delta^{18}O$ studies to model oceanic $\delta^{18}O$ for the present-day (PD) and last glacial maximum (LGM). The model results are analysed in the Atlantic and Arctic, to understand the processes giving rise to the modelled surface and deep oxygen-18 isotope distributions. Sensitivity studies are used to show that the relationship between $\delta^{18}O$ and salinity is not simple, and that the PD $\delta^{18}O$:salinity gradient changed considerably at the LGM.

2. Model details

The OGCM is based on the Southampton–East Anglia (SEA) model, which follows the successful Bryan–Semtner–Cox formulation (Bryan, 1969; Semtner, 1974; Cox, 1984). The model equations are described fully in Beare (1998). It has a free surface formulation for the barotropic mode, adapted to allow the free surface height to respond to the surface fresh water flux. Hence, there is no salt flux across the ocean surface, and salt is exactly conserved in the model. Tracer (temperature, salinity and $\delta^{18}O$) mixing has components in the horizontal, vertical and along isoneutral surfaces (Griffies et al., 1998). The values of the mixing coefficients are taken from England (1993). The topography is constructed from the ETOPO (1986) data set, with sill depths checked using the compilation of Thompson (1995).

The model is implemented on a curvilinear grid, with the model grid's North Pole in Greenland. This enhances model resolution in the North Atlantic and Arctic, and in particular, in the Greenland and Labrador Seas. The OGCM is described in more detail in Wadley and Bigg (2001). The time step length varies across the model domain to allow efficient integration of the variable resolution grid (Wadley and Bigg, 2000). Distorted physics time stepping is used (Bryan, 1984), with a base time step length of 86 400 s for the tracer equations and 5400 s for the momentum equations at all depths.

Seasonal surface forcing is used for momentum, heat and fresh water. For the present-day integration, the wind stress and fresh water fluxes are imposed from climatological values (Hellerman and Rosenstein, 1983; Oberhuber, 1988). An additional 0.2 Sv of fresh water is added uniformly over the Arctic to account for the runoff from surrounding continents (Östlund and Hut, 1984). No other runoff is included directly in the model forcing. The heat flux is derived from restoring to an apparent atmospheric temperature, T^*, with a thermal coupling strength of 15 W

m^{-2} K^{-1}. This surface forcing is described more fully in Wadley and Bigg (2001). There is no sea-ice model, but the insulating effect of sea-ice is accounted for by increasing the sea-surface temperature to -2°C if the surface heat balance results in a lower temperature. Transport of a sea-ice ^{18}O flux is not included in the model.

For the LGM integration, the PD fluxes are adjusted by the addition of a (LGM–PD) wind stress, fresh water flux, and surface air temperature forcing (to T^*), taken from atmospheric model simulations of Dong and Valdes (1998). An additional flux of 1 mm day^{-1} of fresh water between 60°N and 75°N was necessary to obtain a circulation consistent with reconstructions of the LGM ocean circulation, such as that of Boyle (1995).

The OGCM was initialised with climatological temperature (Levitus et al., 1994) and salinity (Levitus and Boyer, 1994) and integrated for 2000 years for both PD and LGM forcing. By this time, the model's thermohaline circulation had settled down to a quasi-steady state, with the model's natural variability showing no trend over time scales longer than 200 years. These circulations were stable for a further 2500 years, during which time the model was run with $\delta^{18}O$ as a passive tracer. This is longer than the thermohaline time scale and allows the isotope distribution to reach quasi-equilibrium with the surface forcing. The present-day circulation is discussed further in Wadley and Bigg (2001).

2.1. $\delta^{18}O$ forcing

In this work, we adopt a physical approach to predict the $\delta^{18}O$ of precipitation and evaporation, but without resorting to the use of $\delta^{18}O$ distributions from atmospheric models with $\delta^{18}O$ as a tracer, such as that of Joussaume and Jouzel (1993). The isotopic composition of precipitation is calculated from the regression formula $\delta^{18}O = -11.88 + 0.345\ T - 0.0022\ P$ (Gat and Gonfiantini, 1981), where T and P are monthly mean temperature (°C) and precipitation (mm $month^{-1}$). It should be noted that the relationship is derived from continental data, and may not be as appropriate over the data-sparse ocean. Precipitation is enhanced in $\delta^{18}O$ by 1.2‰ in the LGM simulations to be consistent with the global oceanic increase used in the model. Global mean salinity is also increased by 1.0 to account for the 120-m change in sea level at the LGM (Fairbanks, 1989).

Evaporation and condensation occur with kinetic fractionation over open water. In agreement with Schmidt (1999) a simple linear resistance model approach is used, which can be written as:

$$R_E = (\alpha_{wv} R_w - h R_a)(1 - K)/(1 - h), \qquad (2)$$

where R_E, R_a and R_w are the isotopic ratios of the evaporating liquid, marine vapour and surface seawater, respectively, $h(=0.75$ everywhere) is the relative humidity and $K = 0.006$ is the kinetic fractionation parameter. The water to vapour fractionation factor, α_{wv}, is given by:

$$\alpha_{wv} = 0.9884 + 1.025 \times 10^{-4} T - 3.57 \times 10^{-7} T^2, \qquad (3)$$

(Gat and Gonfiantini, 1981), where T (in Celsius) is the mean monthly climatological air temperature. The use of observed relative humidity in Eq. (2) instead of a constant 0.75, resulted in unrealistic surface isotope values in regions of high relative humidity. This is due to the $1/(1-h)$ term in Eq. (2). Relative humidity was therefore set to 0.75.

In the LGM simulation, the (LGM–PD) temperature difference (Dong and Valdes, 1998) is added in Eq. (3). R_a is taken to have the $\delta^{18}O$ value of the local precipitation, minus 9‰, consistent with the global offset (Gat, 1996). R_E is then converted to a $\delta^{18}O$ value using Eq. (1).

The 0.2 Sv addition of fresh water to the Arctic is given a $\delta^{18}O$ value of -21‰ in both the PD and LGM simulations. (This is changed to -42‰ in sensitivity experiments.) For each surface grid cell, the precipitation, evaporation and runoff are summed to produce a single fresh water addition (or loss) to the surface of the modelled ocean, with a $\delta^{18}O$ value consistent with conservative mixing of the three components. The fresh water addition to the surface of the modelled ocean is then mixed conservatively with the oceanic water in the top model level to represent the oceanic surface forcing of $\delta^{18}O$. This method of surface $\delta^{18}O$ forcing does not automatically conserve $\delta^{18}O$ in the ocean. The global flux was, therefore, calculated each model time step, and a globally uniform adjustment made to the $\delta^{18}O$ flux associated with the local fresh water flux, to force the global integrated surface flux to be zero. This correction had a globally integrated annual mean value of -1.2 ‰ Sv for the PD control simulation, and -1.3 ‰ Sv for the LGM control simulation.

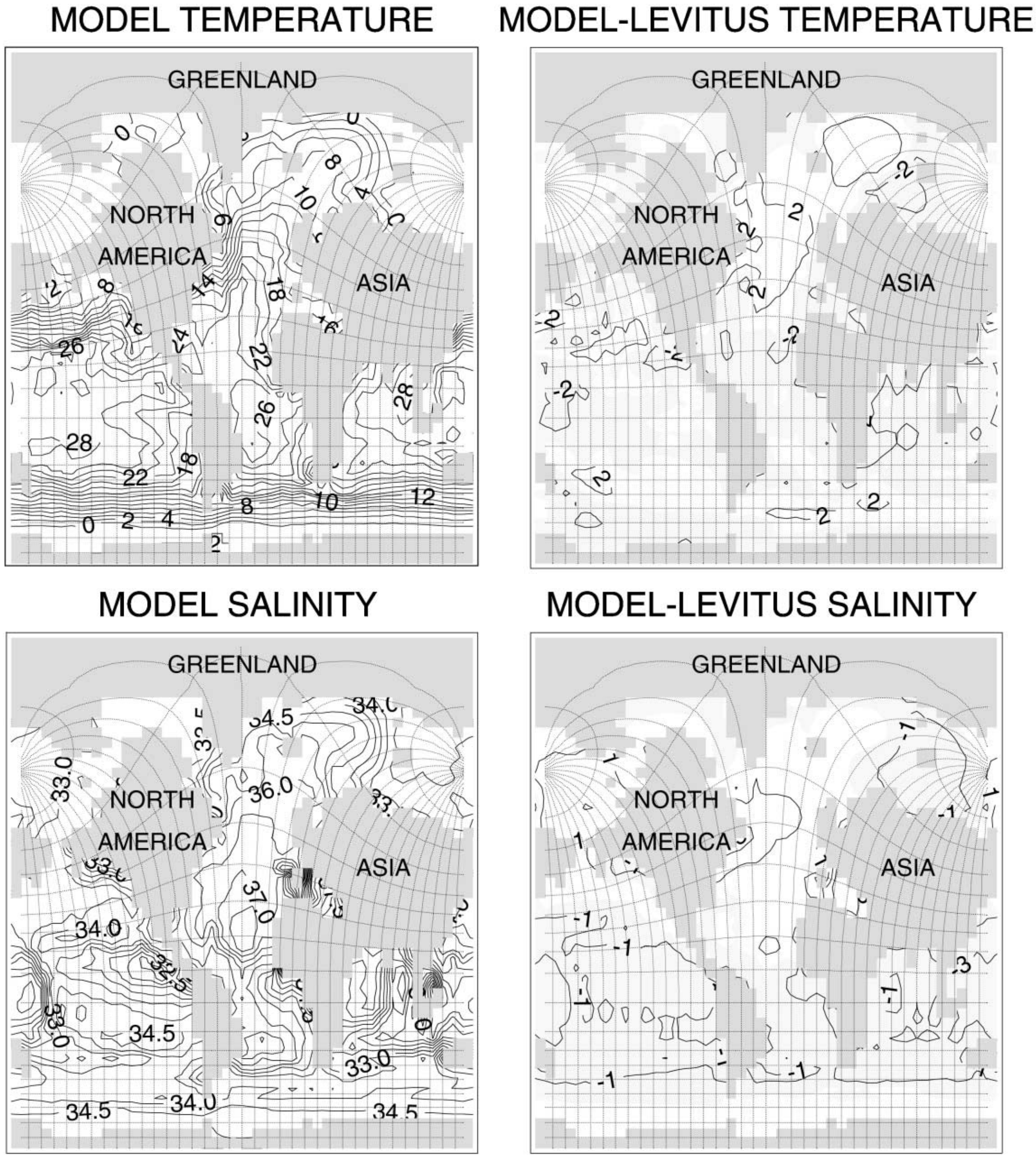

Fig. 1. Top: annual mean present-day modelled surface temperature (left) and modelled minus climatological surface temperature (right), averaged over years 4000–4500. The shaded areas are where the modelled temperature is less than the climatological temperature. Bottom: same for salinity. The climatological fields are from Levitus et al. (1994) for temperature, and Levitus and Boyer (1994) for salinity. The contour interval is 2 °C for temperature, and 0.5 for salinity (1 in the difference plot). Note the projection used in the model has the model North Pole in Greenland. Lines of equal latitude and longitude are shown at intervals of 10°.

3. Modelled oceanic circulation

Results from the PD simulation are discussed in detail in Wadley and Bigg (2001). Here, the key features of the circulation will be presented, together with the corresponding LGM modelled circulation.

The PD modelled circulation is reasonably consistent with that observed. Fig. 1 shows the annual mean modelled sea surface temperature, and its difference from the Levitus et al. (1994) climatology. Temperatures are generally within 2°C of those observed. The North Atlantic is generally too warm, whereas low latitudes are too cool. Surface salinities are also too high in the North Atlantic, and too low at low latitudes. This leads to the modelled North Atlantic deep water (NADW) being warmer and saltier than that observed. Conservation of salt in the model requires a reduction in salinity of other water masses, and this occurs mainly in the upper 1000 m of the Pacific and Indian Oceans. Antarctic intermediate water penetrates into the Pacific, Atlantic and Indian Oceans, but does not extend as far northward as observed. In the Atlantic, the overturning circulation has a peak transport of 25 Sv, and exports 16 Sv south of 34°S, consistent with previous observations (Gordon, 1986; Schmitz, 1995) (Fig. 2). Beneath this, 6 Sv of Antarctic bottom water enters the South Atlantic, also consistent with previous observations (Speer and Zenk, 1993). The exchanges between the North Atlantic and Nordic Seas also agree well with those observed (Wadley and Bigg, 2001). The modelled volume flux through the Bering Strait is 1.8 Sv, greater than the 0.8 Sv previously observed (Coachman and Aagaard, 1988). The Antarctic circumpolar current has a strength of 165 Sv, somewhat higher than observed (130–140 Sv) (Nowlin and Klinck, 1986).

Fig. 3 shows the LGM modelled surface temperature and its difference from the PD modelled values. The greatest cooling is over the North Atlantic, where the North Atlantic current takes a more southerly path. The Southern Ocean has also cooled by up to 4°C. In the low-latitude Pacific, modelled sea surface temperatures are higher at the LGM than the PD. This is due to the imposition of CLIMAP (1981) sea surface temperatures in the atmospheric GCM, from which

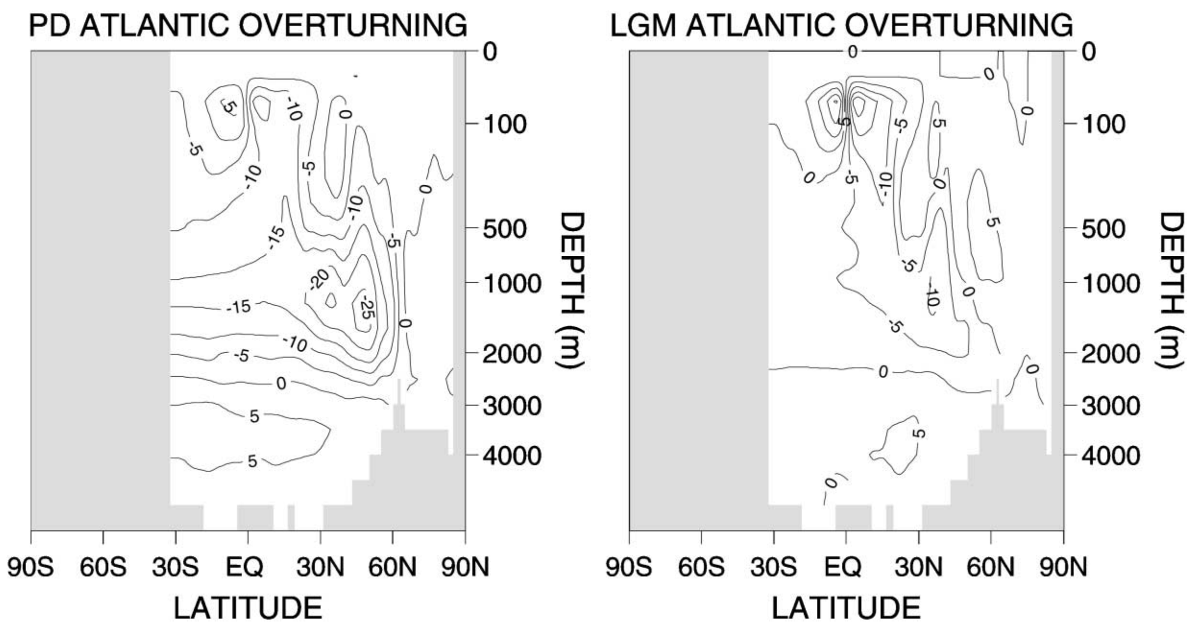

Fig. 2. Overturning stream function in the Atlantic averaged over years 4000–4500, for the present-day (left) and last glacial maximum (right). The contour interval is 5 Sv. Note the non-linear depth scale.

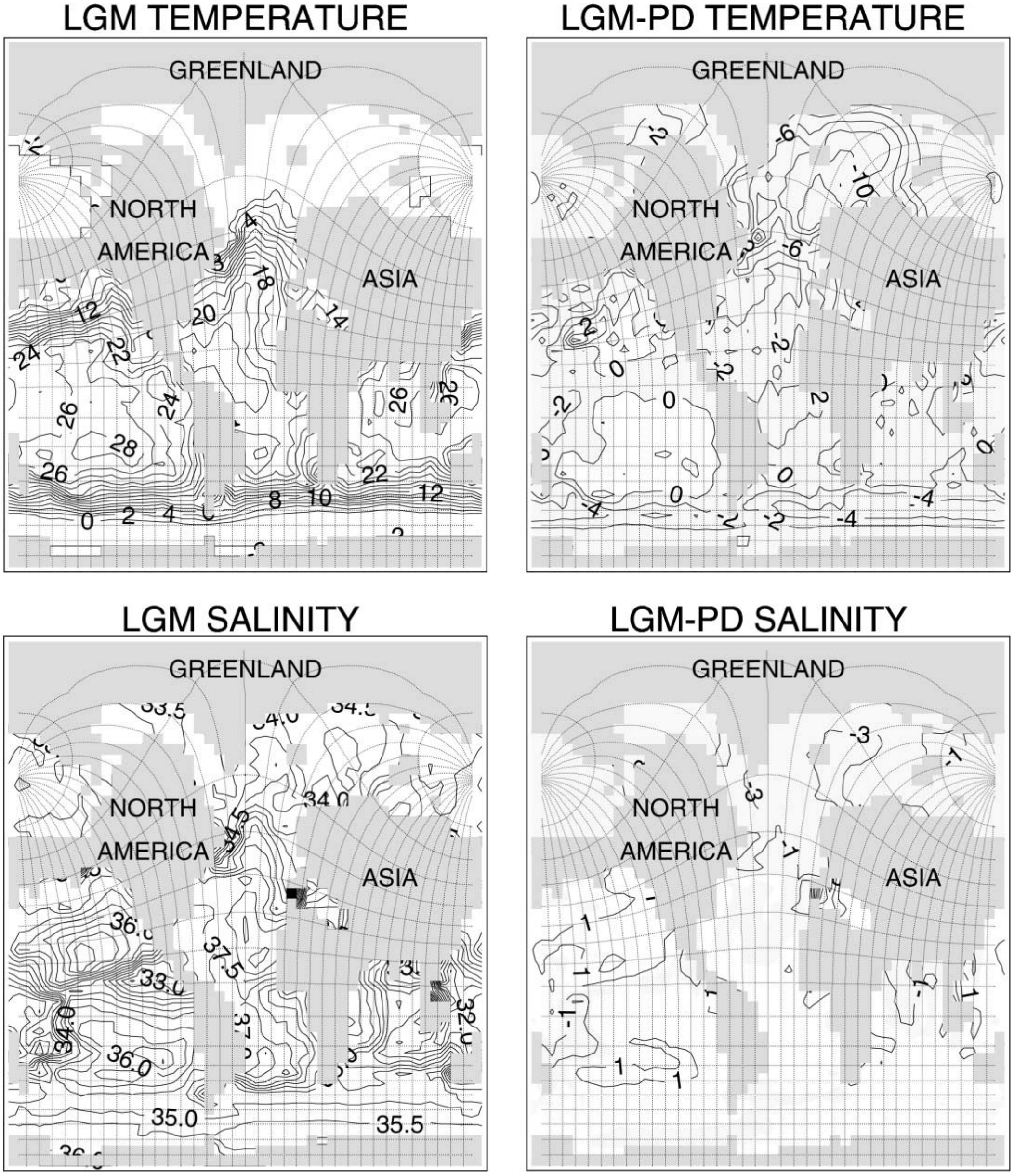

Fig. 3. Top: Annual last glacial maximum modelled surface temperature (left) and modelled minus present-day surface temperature (right), averaged over years 4000–4500. The shaded areas are where the present-day temperature is less than the last glacial maximum temperature. Bottom: same for salinity. The contour interval is 2 °C for temperature, and 0.5 for salinity (2 in the difference plot).

the forcing fields were derived. Between 30° and 40°N in the Pacific, there is also an increase in surface temperature. This is associated with convection to 500 m depth, but does not contribute to intermediate-level water properties far beyond the convective region. The weaker northward flow in the Atlantic associated with the thermohaline circulation advects less salt northwards. This reduces the modelled surface salinities by up to 3 in the northern North Atlantic and Arctic (Fig. 3). Surface salinities elsewhere are generally within 1 of the PD values (allowing for the increase of 1 at the LGM). The overturning in the Atlantic has changed significantly from the PD (Fig. 2). The convective zone has moved southward to 40–50°N, and reduced in strength to 10 Sv, less than half the PD strength. Only 4 Sv leaves the Atlantic at 30°S, with the remainder upwelling in the North Atlantic. Below 2500 m, 4 Sv of Antarctic bottom water enters from the south, less than at the PD.

This model-derived LGM ocean circulation is broadly consistent with that suggested from proxy reconstructions. A LGM circulation with NADW sinking to intermediate depth and feeding into the circumpolar deep water of the Southern Ocean, but with the deep water of all ocean basins dominated by southern source water has been proposed by Boyle (1995), and is currently gaining widespread support. Our modelled export of only 4 Sv of glacial NADW is consistent with this, although the depth of the overturning cell associated with NADW formation is similar in both the PD and LGM simulations. A much reduced export of North Atlantic source water at the LGM is also a feature of the coupled model of Ganopolski et al. (1998), although their maximum meridional overturning strength remains unchanged from the corresponding PD simulation. Our model has some "ice-free" water in the Nordic Seas in summer (not shown), consistent with reconstructions (Veum et al., 1992; Hebbeln et al., 1994; Sarnthein et al., 1995). However, it is not thought that there was a significant export of dense water originating in this area to the Atlantic proper (Labeyrie et al., 1992; Sarnthein et al., 1995). This is also the case in the model. Deep convection occurs in the model south of the Greenland–Scotland Ridge, mainly between Greenland and Iceland.

4. Oxygen isotope modelling

4.1. Present-day

Fig. 4 shows the PD climatological surface $\delta^{18}O$, from Bigg and Rohling (2000), modelled surface $\delta^{18}O$, and the difference between the modelled and climatological fields. The climatological field shows generally high $\delta^{18}O$ values at low latitudes, and low values at high latitudes. The sub-tropical enrichment reflects high evaporation, which preferentially removes the lighter $H_2{}^{16}O$ molecules from the sea surface, whereas precipitation depleted in $H_2{}^{18}O$, results in low $\delta^{18}O$ values at high latitudes. This general trend is also present in the modelled surface distribution, but differences also exist. In the Arctic Ocean, climatological values are considerably lower than in the model. This is also the case in the Labrador Sea, due to flow through the Canadian Archipelago advecting $\delta^{18}O$ properties from the Arctic. The climatology shows high $\delta^{18}O$ in the western tropical Atlantic, which is not present in the modelled field. This is associated with numerical extrapolation from point values in the western Atlantic and is probably artificially high. A decrease in relative humidity in the model could compensate for this difference. Modelled $\delta^{18}O$ values in the North Pacific are too high. The modelled values here were found to be very sensitive to the imposed relative humidity, and decreased as relative humidity was increased from the imposed 75%, indicating that a higher value should be used in this region, consistent with the climatology of Gorshkov (1978).

Examination of the relationship between $\delta^{18}O$ and salinity helps to explain the surface distributions of $\delta^{18}O$. Atlantic $\delta^{18}O$:salinity data from Bigg and Rohling (2000) are shown in Fig. 5, with the model results in Fig. 6, for all depths. The climatology shows a general increase in $\delta^{18}O$ with salinity, with a gradient of ~ 0.6 at lower latitudes, but a steeper gradient at higher latitudes. The gradient of 0.6 is associated with mixing of Arctic runoff with NADW. There is, however, a near-horizontal line between equatorial and low-latitude points, which is evident in the model results. There is also a vertical line of points with a salinity of 34.9 — the salinity of NADW, showing the variability of the $\delta^{18}O$ measured in this water mass.

The modelled $\delta^{18}O$:salinity relationship shows less scatter than the climatology (Fig. 6). This is partially because of the absence of interannual variability in the forcing of the model. The highest salinity (and $\delta^{18}O$) points are found in the surface low-latitude Atlantic, whereas the lowest salinity points are from the surface Arctic waters. There is also a water type with low salinity, but not-so-low $\delta^{18}O$, which origi-

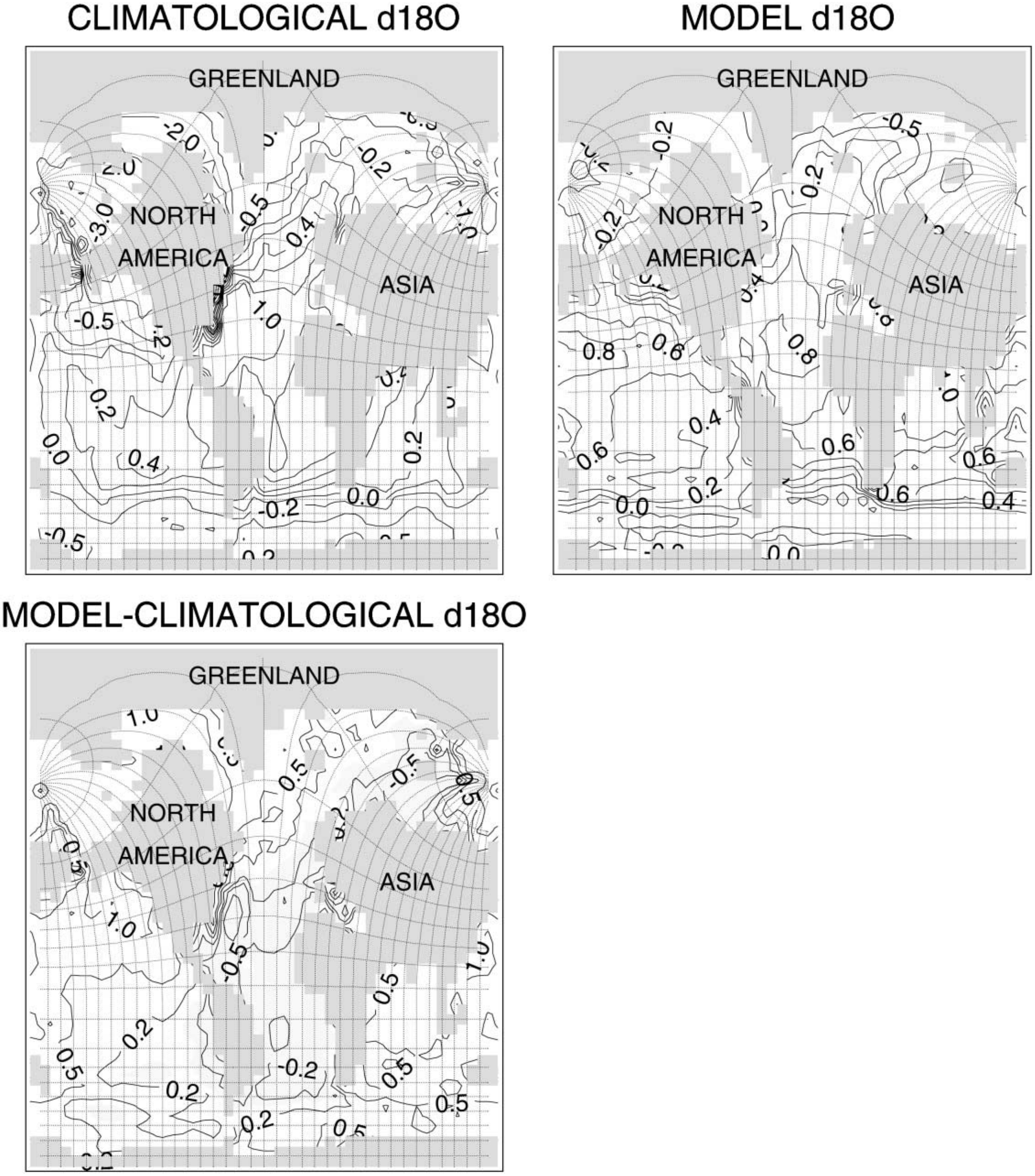

Fig. 4. Present-day climatological (top left), modelled (top right) and modelled minus climatological (bottom) surface $\delta^{18}O$ distributions. The climatological field is from Bigg and Rohling (2000). The shaded areas are where the modelled $\delta^{18}O$ is lower than in the climatology. Note the non-uniform contour interval in the Arctic in these plots.

nates in the Labrador Sea model. Recent work has shown that Labrador Sea water has a sea-ice deficit of about 250 km^3 $year^{-1}$, which enhances its salinity, but not its $\delta^{18}O$ (Frew et al., 2000). The absence of a sea-ice model in our simulations causes Labrador Sea water to be too fresh, and accounts for the displacement of the Labrador Sea values from the main $\delta^{18}O$:salinity line. The modelled mixing of water properties from the low-latitude Atlantic with Arctic waters occurs with a $\delta^{18}O$:salinity gradient of 0.35

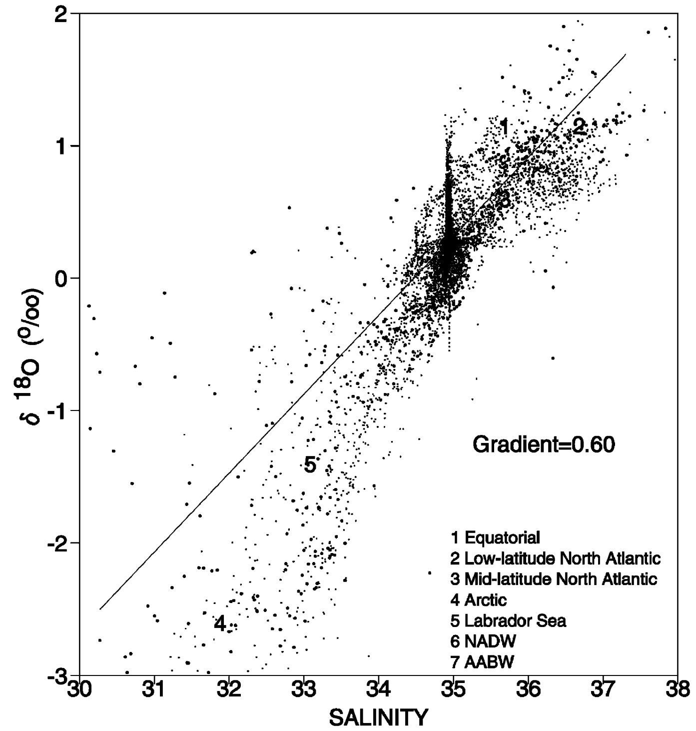

Fig. 5. Atlantic $\delta^{18}O$ vs. salinity from the present-day climatology of Bigg and Rohling (2000). The line with gradient 0.60 has the gradient associated with mixing of Arctic runoff with NADW. The larger dots are for values in the top 30 m. A few points with high $\delta^{18}O$ values from the Mediterranean are not shown. This is also the case in Figs. 6, 8, 9, 10, 11 and 12. See text for more details.

(Fig. 6). The corresponding observed line, with a gradient of ~ 0.6, is consistent with the mixing of subtropical Atlantic water with fresh water runoff to the Arctic, which has a $\delta^{18}O$ value of − 21‰ (Östlund and Hut, 1984). This line also passes through the properties of NADW (0.2‰, 34.9). In a previous oceanic modelling study, Schmidt (1998) found a $\delta^{18}O$:salinity gradient of 0.46 in the Atlantic, which was attributed to a poor representation of the thermohaline circulation. However, we believe the reason for the difference between the modelled and observed $\delta^{18}O$:salinity relationships is as follows.

The modelled mixing line has the much-smaller gradient of 0.35, despite the model having an input of 0.2 Sv of runoff to the Arctic with a $\delta^{18}O$ of − 21‰. There are also precipitation and evaporation fluxes to the Arctic, which give a total input of 0.26 Sv, with a net $\delta^{18}O$ of − 19.5‰. This can be explained by also considering the inflow to the Arctic through the Bering Strait. Both this inflow, and the runoff, must be exported southward to, and through, the Atlantic. Thus, the mixing of low-latitude Atlantic water occurs with the mixture of these two inputs, not just the runoff. As we have already seen, the modelled input through the Bering Strait is stronger than observed. Taking the mixture of 1.8 Sv of modelled Bering Strait inflow, ($\delta^{18}O$ = 0.0‰, salinity = 33 (but note the observed $\delta^{18}O$ = −1.0‰)), and 0.26 Sv of runoff, precipitation and evaporation ($\delta^{18}O$ = − 19.5‰, salinity = 0.0), gives 2.06 Sv of water with $\delta^{18}O$ = − 2.46‰ and salinity = 28.8. The gradient of a mixing line of this, with modelled NADW[1]

[1] NADW is used as the end-member because it is the ultimate fate of waters entering the North Atlantic from both the north and south. As an extensive water mass, its properties are close to VSMOW, but it is a more appropriate end-member for understanding processes in the North Atlantic.

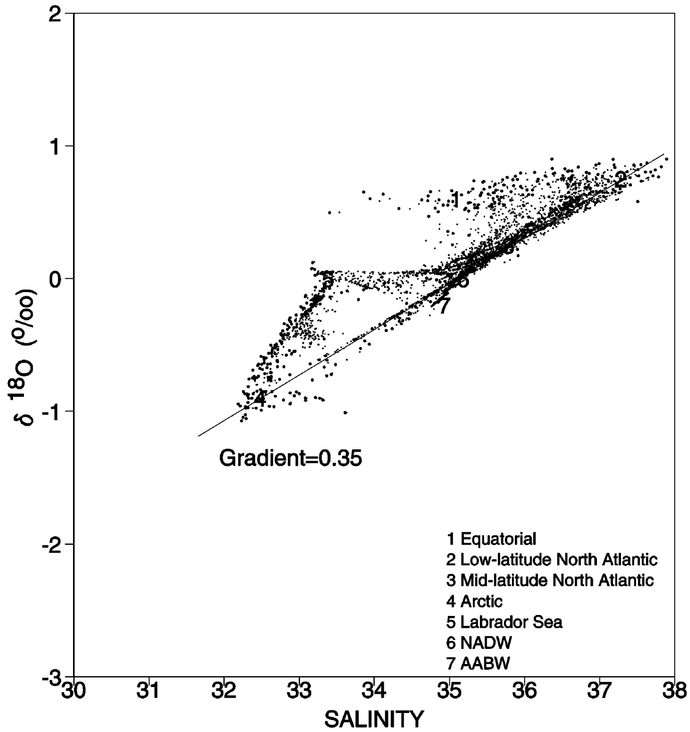

Fig. 6. Atlantic $\delta^{18}O$ vs. salinity for the present-day control simulation. See text for more details.

($\delta^{18}O = 0.0$ ‰, salinity = 35.2) is $(0.0-(-2.46))/(35.2-28.8) = 0.38$, in good agreement with the modelled mixing line gradient of 0.35 (Fig. 6). Without accounting for the Bering Strait inflow, the expected gradient would be $(0.0-(-19.5))/(35.2-0.0) = 0.55$, which is not compatible with the model gradient. Thus the $\delta^{18}O$ of the modelled inflow to the Atlantic is controlled by both the runoff to the Arctic, and inflow through the Bering Strait.

So what impact does the Bering Strait inflow have on the North Atlantic $\delta^{18}O$:salinity relationship in the real ocean? Bering Strait inflow water ($\delta^{18}O = -1.0$ ‰ (Bigg and Rohling, 2000), salinity = 33 (Levitus and Boyer, 1994)), differs from NADW ($\delta^{18}O = 0.2$ ‰, salinity = 35.2) with a $\delta^{18}O$:salinity gradient of 0.55, whereas runoff ($\delta^{18}O = -21$ ‰, salinity = 0.0), differs by a $\delta^{18}O$:salinity gradient of 0.60. Thus, Bering Strait water lies close to the $\delta^{18}O$:salinity mixing line between Arctic meteoric water and NADW. The correspondence with the results of the modelled ocean suggests that previous explanations of the observed $\delta^{18}O$:salinity gradient involving only an Arctic runoff end-member have overlooked the Bering Strait contribution.

The contribution of the Bering Strait also explains the high modelled $\delta^{18}O$ values in the Arctic. In the real Arctic Ocean, physical separation of the Bering Strait water from the runoff allows the very low $\delta^{18}O$ runoff to retain its identity in the surface waters. In the model, coarse resolution and the spatially uniform addition of runoff to the Arctic Ocean causes mixing between the Bering Strait inflow and runoff inputs, giving higher surface $\delta^{18}O$ values than observed. The $\delta^{18}O$ of the modelled Bering Strait inflow is also higher than observed, but this is of secondary importance, when compared with the model's inability to separate the Bering Strait inflow from the very $\delta^{18}O$-depleted fresh water input in the Arctic Ocean.

4.2. Last glacial maximum

The modelled LGM surface $\delta^{18}O$ distribution is shown in Fig. 7. To account for preferential removal of $H_2{}^{16}O$ to glacial ice sheets, 1.2 ‰ was added to

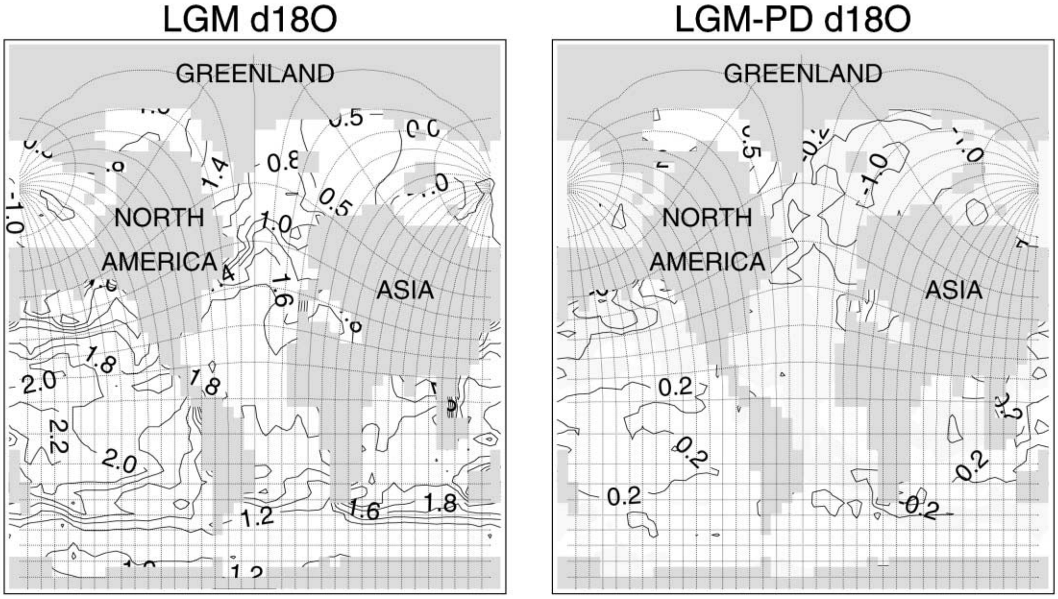

Fig. 7. Last glacial maximum (left) and last glacial maximum minus present-day minus 1.2‰ (right) surface $\delta^{18}O$ distributions. The shaded areas are where the last glacial maximum $\delta^{18}O$ is lower than in the present-day in the simulations. Note the non-uniform contour interval in these plots.

the global mean $\delta^{18}O$. Allowing for the 1.2‰ offset, surface values in the Pacific, Indian and Southern Oceans are broadly similar to the modelled PD, but more significant differences exist in the Atlantic. The Atlantic has lower surface $\delta^{18}O$, especially in the Nordic Seas. This is due to the southward movement of the North Atlantic Current at the LGM, and redirection of Atlantic water, with its high $\delta^{18}O$, away from the Nordic Seas. At lower latitudes, surface $\delta^{18}O$ is also slightly lower at the LGM, due to a weaker overturning circulation (Fig. 2), lower northward heat transport, and therefore, evaporation and removal of ^{16}O by evaporation.

In this simulation, runoff to the Arctic has the same $\delta^{18}O$ value and volume flux as in the PD simulation, and is therefore not directly responsible for the low surface Arctic $\delta^{18}O$. The key difference is the closed Bering Strait and Canadian Archipelago connections, due to the lowering of sea level at the LGM (Fairbanks, 1989) and the ice-locked Nares Strait (Zreda et al., 1999). In the PD simulation, inflow from the Pacific dilutes the Arctic runoff, whereas without this inflow surface, $\delta^{18}O$ values fall to -1.0‰ (i.e. -2.2‰ when compensated for the 1.2‰ global offset), closer to the typical observed values for the PD (Fig. 4).

The LGM relationship between $\delta^{18}O$ and salinity is shown in Fig. 8. $\delta^{18}O$ increases with salinity in the region south of 55°N with a gradient of 0.22, considerably lower than the 0.35 seen in the PD simulation, and the ~ 0.6 observed for the PD. The $\delta^{18}O$:salin-O:salinity gradient is steeper in the Nordic and Arctic Seas, but the Labrador Sea has high $\delta^{18}O$, low salinity water. There is no runoff to the Labrador Sea in the model, which would supply fresh water depleted in $\delta^{18}O$, and no increase in salinity due to sea-ice formation (see PD control experiment). This, combined with the absence of $\delta^{18}O$-depleted Arctic water via the Canadian Archipelago, and very low precipitation, accounts for the high $\delta^{18}O$ in the Labrador Sea. Runoff would almost certainly have resulted in lower $\delta^{18}O$ at the LGM, but the high $\delta^{18}O$ in the absence of runoff suggests that $\delta^{18}O$ records in the Labrador Sea may strongly reflect changes in local runoff. The fresh water runoff to the Arctic provides the only significant input to the Atlantic basin north of the latitude of glacial North Atlantic deep water (GNADW) formation. The lower

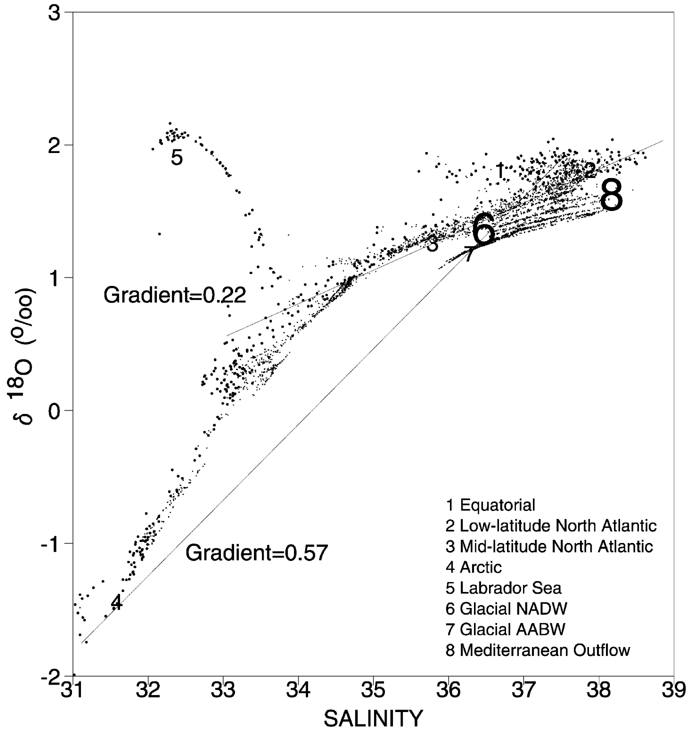

Fig. 8. Atlantic $\delta^{18}O$ vs. salinity for the last glacial maximum control simulation. See text for more details.

precipitation and evaporation in the Arctic at the LGM gives a net input of 0.22 Sv with $\delta^{18}O = -21$ ‰. If this fresh water input becomes incorporated into GNADW, we would expect the Arctic to lie on a line in $\delta^{18}O$:salinity space through GNADW ($\delta^{18}O = 1.3$ ‰, salinity = 36.5), with a gradient of $(1.3-(-21))/(36.5-0.0)=0.61$. A mixing line from the most $\delta^{18}O$-depleted Arctic waters to the GNADW has a gradient of 0.57, in agreement with this. Note, however, that mixing of this Arctic water with mid-Atlantic and Labrador Sea water prior to GNADW formation results in the $\delta^{18}O$:salinity relationship being displaced from this line. On the higher salinity side of GNADW (point 6 in Fig. 8), the mixing line between GNADW and Mediterranean outflow water has a similar gradient to the low → mid-latitude $\delta^{18}O$:salinity gradient, but is offset to a lower $\delta^{18}O$, giving distinct mixing lines below the surface mixing line (from 6 to 8, in Fig. 8). The Mediterranean outflow water is sufficiently dense to sink to over 4000 m, and also mixes with glacial Antarctic bottom water (GAABW) (from 7 to 8, in Fig. 8). These distinct mixing lines correspond to individual vertical levels in the model, and therefore, would not be expected in the real ocean. The higher salinity arm of the $\delta^{18}O$:salinity relationship is, therefore, set by a subtle balance between the surface flux of $\delta^{18}O$ (from 2 to 6, in Fig. 8), fresh water, and oceanic advection and mixing.

5. Sensitivity experiments — increased depletion of $\delta^{18}O$ in Arctic runoff

5.1. Present-day

The extensive ice sheets of the LGM would be likely to supply runoff very depleted in $\delta^{18}O$ to the Arctic and Northern Atlantic. To test our model's sensitivity to this, the PD and LGM simulations were rerun with the Arctic runoff $\delta^{18}O$ set to -42 ‰, for 4500 years, as in the control runs. This PD simulation can be thought of as an analogue for the period around 10,000 years ago, when the Bering Strait and

Canadian Archipelago seaways were opening as sea levels rose, but there were still inputs of highly depleted-δ^{18}O runoff from the melting ice sheets. Fig. 9 shows the δ^{18}O:salinity relationship for the PD with this change to the forcing. The net Arctic inflow now consists of 0.26 Sv of runoff with $\delta^{18}O = -35.7$‰, salinity = 0.0, and an unchanged 1.8 Sv of Bering Strait inflow with $\delta^{18}O = 0.0$‰, salinity = 33, giving a net input of 2.06 Sv with $\delta^{18}O = -4.5$‰, salinity = 28.8. The gradient between this and NADW is $(0.0-(-4.5))/(35.2-28.8) = 0.70$. The modelled δ^{18}O:salinity relationship shows mixing between the most depleted Arctic water and Nordic Sea waters with a gradient of 0.67 and mixing between the most δ^{18}O-depleted Arctic water and NADW, with a gradient of 0.72, consistent with the mixing argument. The reduction of the δ^{18}O of the Arctic runoff changes neither the low-latitude surface Atlantic properties, nor those of NADW, but bends the mixing line between them towards lower δ^{18}O, as a result of mixing with the Arctic water. The Labrador Sea properties have not changed, showing that in the model, it is the Bering Strait inflow which is setting the δ^{18}O values of the southward flow through the Canadian Archipelago. It is not, however, possible to conclude that this is the case in the real ocean, due to the strong Bering Strait inflow and coarse grid used in the model. This experiment shows that the linear δ^{18}O:salinity relationship seen in the PD control simulation hides a more complex picture of mixing between water masses in the Atlantic.

5.2. Last glacial maximum

Fig. 10 shows the corresponding δ^{18}O:salinity relationship for the LGM experiment with δ^{18}O-depleted Arctic runoff. Runoff to the Arctic was likely to be more depleted in δ^{18}O at the LGM than today, due to the input of glacier-derived meltwater, which is depleted in δ^{18}O due to the altitude at which the precipitation falls over high ice sheets. The reduction in Arctic runoff δ^{18}O to -42‰ is consistent with the mean δ^{18}O of glacial ice at the LGM (Fairbanks

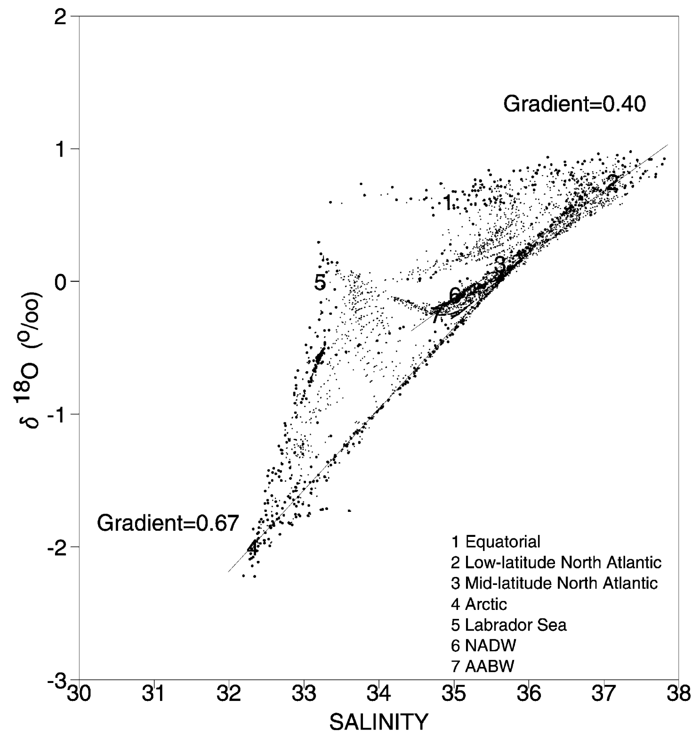

Fig. 9. Atlantic δ^{18}O vs. salinity for the present-day simulation with increased depletion of δ^{18}O in Arctic runoff. See text for more details.

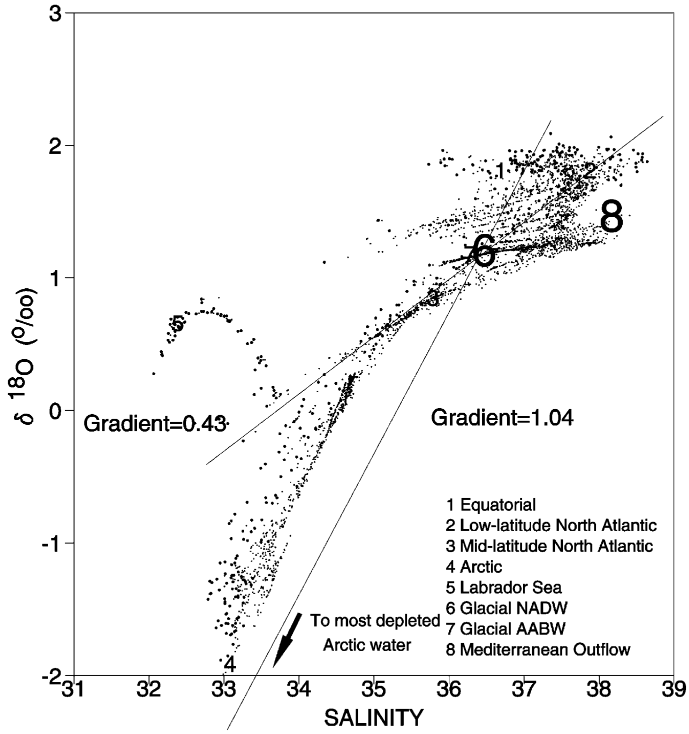

Fig. 10. Atlantic $\delta^{18}O$ vs. salinity for the last glacial maximum simulation with increased depletion of $\delta^{18}O$ in Arctic runoff. See text for more details.

and Matthews, 1978). The volume input of 0.2 Sv is, however, rather larger than estimates would suggest. Bigg and Wadley (2001) estimated that 0.03 Sv of glacial ice entered the Arctic during the LGM, and that a total of 0.10 Sv of glacial ice/meltwater entered the North Atlantic. The $\delta^{18}O$:salinity relationship (in the absence of Bering Strait inflow) is not dependent on the volume flux of meteoric water, but its $\delta^{18}O$ signature, so the following analysis is still representative of the real LGM situation. It is therefore important to determine the sensitivity of the $\delta^{18}O$:salinity relationship to the $\delta^{18}O$ of Arctic runoff, so that the accuracy of palaeoclimate reconstructions based on oceanic $\delta^{18}O$ values can be assessed. The net input to the Arctic, including precipitation and evaporation, is now $\delta^{18}O = -40.0$ ‰. In the absence of Bering Strait inflow at the LGM, the gradient of the mixing line between this and GNADW is $(1.2-(-40.0))/(36.4-0.0)=1.13$. The modelled mixing line has a gradient of 1.04, close to that predicted. As in the control simulation, points do not lie on this line due to prior mixing with mid-Atlantic and Labrador Sea waters. The high $\delta^{18}O$/low salinity Labrador Sea water mixes with North Atlantic water, moving the mixing line towards higher $\delta^{18}O$/low salinity.

The GNADW and glacial Antarctic bottom water (GAABW) points reduce in $\delta^{18}O$ by 0.15 ‰ with the Arctic runoff $\delta^{18}O$ of -42 ‰. In the corresponding PD simulation, this is not the case. This is because of the constraint of global conservation of $\delta^{18}O$ in the ocean model. In the PD circulation, NADW leaves the Atlantic and is present in much of the deep global ocean. Any change in its $\delta^{18}O$ content must be compensated for by changes in other water masses. The modelled GNADW has a much weaker exchange with the rest of the ocean, and therefore, occupies a much smaller proportion of the ocean's volume. Therefore, changes in its $\delta^{18}O$ content can be accommodated with only small changes in the $\delta^{18}O$ of other (southern source) water masses. This experiment shows that

LGM $\delta^{18}O$ distributions in the North Atlantic may be much more sensitive to changes in forcing than at the PD, with implications for the reconstruction of climate at the LGM.

6. Sensitivity experiments — the role of oceanic advection

The previous experiments have shown that the low- and mid-latitude relationships between $\delta^{18}O$ and salinity depend not only on mixing between the most enhanced and depleted sources of $\delta^{18}O$, but on a local balance between surface $\delta^{18}O$ flux and oceanic advection and mixing, confirming the arguments of Rohling and Bigg (1998). If this is *not* the case, changing the rate of advection of $\delta^{18}O$ should have no effect on the $\delta^{18}O$:salinity relationship. Accordingly, the model was rerun for both the PD and LGM, with the oceanic advection of $\delta^{18}O$ doubled. The horizontal and vertical advection terms for the $\delta^{18}O$ equation were multiplied by a factor of two, except for the vertical advection term at the top of the surface grid box, to keep the surface flux of $\delta^{18}O$ unchanged. This has no physical analogue in the real ocean, but is designed to explore the physical processes controlling the $\delta^{18}O$ distributions.

6.1. Present-day

Fig. 11 shows the PD $\delta^{18}O$:salinity relationship for the Atlantic in this experiment. The impact of the Bering Strait inflow has now been changed, because there is twice as much $\delta^{18}O$ being advected into the Arctic from the Pacific. The net inflow to the Arctic now consists of 0.26 Sv of runoff with $\delta^{18}O = -19.5$ ‰, salinity = 0 and 2×1.8 Sv of Bering Strait inflow, with $\delta^{18}O = 0.0$ ‰, salinity = 33, giving a net input with $\delta^{18}O = -1.31$ ‰, salinity = 28.8. The gradient between this and modelled NADW is $(0.0-(-1.31))/(35.2-28.8) = 0.20$, in agreement with the 0.20 in the model (Fig. 11). This is considerably less than in the case of the control model (0.35), showing that oceanic advection of $\delta^{18}O$ through the Bering

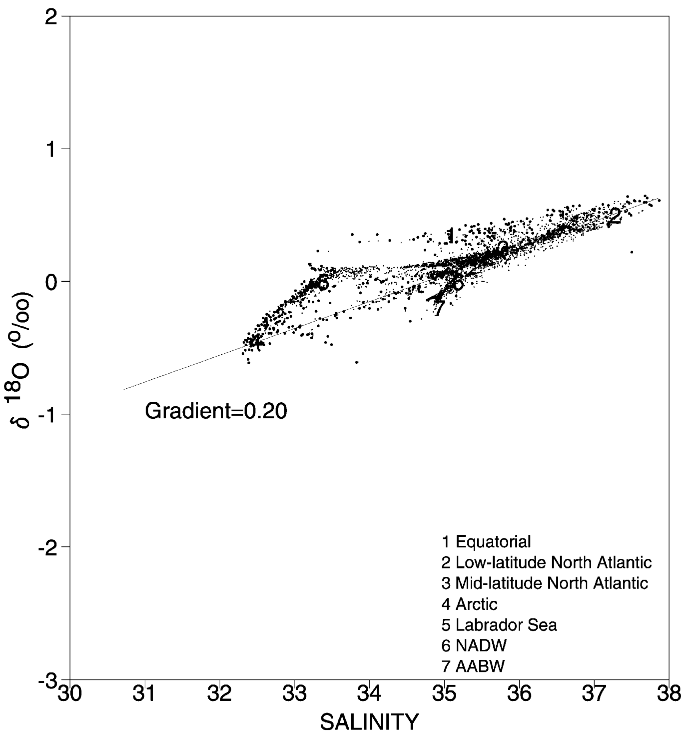

Fig. 11. Atlantic $\delta^{18}O$ vs. salinity for the present-day simulation with doubled advection of $\delta^{18}O$. See text for more details.

Strait plays a key role in determining the high-latitude δ^{18}O:salinity gradient.

The surface waters in the low- and mid-latitude North Atlantic now also exhibit a gradient of 0.20, half that in the control simulation. This is not due to mixing with the δ^{18}O-depleted Arctic inflow, as this has been shown to have little impact on the low/mid-latitude δ^{18}O:salinity relationship in the experiment with δ^{18}O-depleted runoff to the Arctic. It is the doubling of the oceanic advection of δ^{18}O which has halved the gradient of the δ^{18}O:salinity line, by doubling the supply of δ^{18}O to balance the surface flux. This part of the δ^{18}O:salinity relationship is, thus, not a mixing line, but is set up by a balance between the surface flux and oceanic advection.

6.2. Last glacial maximum

The LGM δ^{18}O:salinity relationship for the doubled advection experiment is shown in Fig. 12. There is no inflow through the Bering Strait, so the net Arctic inflow is unchanged from the control simulation. The GNADW remains virtually unchanged in δ^{18}O properties, consistent with conservation of δ^{18}O in the Atlantic system as a whole, since these waters account for most of the volume in the Atlantic, and there is little exchange with the underlying Antarctic source water. The gradient of a line in δ^{18}O:salinity space joining GNADW and Arctic surface waters reduces from 0.57 to 0.34, which is the same ratio as the present-day reduction. Thus, the rate of Arctic advective ventilation of δ^{18}O is important in determining the Arctic δ^{18}O concentration. This must also contribute to the changes in the PD simulation above. In the LGM control simulation, the low- and mid-latitude surface waters lie on a line with a 0.22 gradient, whereas now the gradient is 0.14, slightly more than half the gradient in the control run. This contrasts with the PD case, where both these mixing gradients halved. The explanation lies in the relatively closed circulation in the LGM North Atlantic. In the PD case, the circulation consists of an upper level inflow from

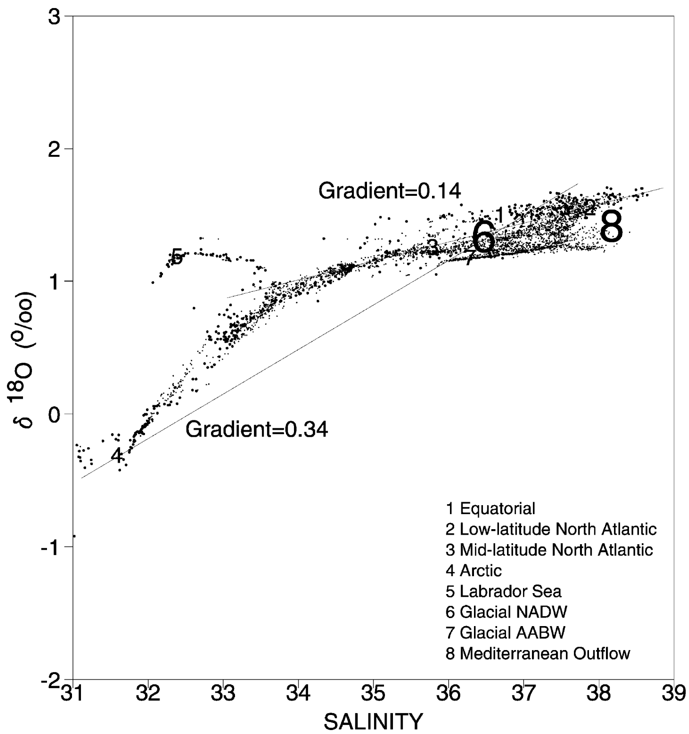

Fig. 12. Atlantic δ^{18}O vs. salinity for the last glacial maximum simulation with doubled advection of δ^{18}O. See text for more details.

the south and return flow beneath, with a large upstream reservoir of water properties. Doubling the rate of oceanic advection of $\delta^{18}O$ through this system cuts the change of $\delta^{18}O$ concentration in half as fluid moves through the system. At the LGM, however, the water is mostly recirculating around the North Atlantic, with much reduced exchange with the other oceans. Hence, the intermediate and deep waters formed in the North Atlantic upwell to modify the low-latitude surface waters. Changes in circulation in this closed system can result in large and spatially complex changes in surface $\delta^{18}O$ distributions, making interpretation of changes in $\delta^{18}O$ records from oceanic cores much more difficult.

7. Discussion

A global ocean GCM has been run to equilibrium with oxygen isotopes for the PD and LGM. Integrating to equilibrium, in conjunction with global conservation of $\delta^{18}O$, ensuring that the modelled surface $\delta^{18}O$ distribution is in equilibrium with surface forcing, and also with the surface and thermohaline circulation, unlike simulations of decadal time scale (Schmidt, 1998).

The Bering Strait flux has been shown to affect the North Atlantic $\delta^{18}O$:salinity relationship. Based on observations of salinity (Levitus and Boyer, 1994) and $\delta^{18}O$ (Bigg and Rohling, 2000) in the Bering Strait, and the $\delta^{18}O$ composition of runoff to the Arctic (Östlund and Hut, 1984), it is seen that the observed inflow through the Bering Strait lies on a line in $\delta^{18}O$:salinity space joining Arctic meteoric water with NADW. This means that the observed northern North Atlantic $\delta^{18}O$:salinity gradient of 0.6 is caused by both of these inputs, but would still be present if one input were removed. The coincidence of the Bering Strait inflow/NADW and Arctic meteoric water/NADW mixing lines in *observed* data is probably due to the similar latitudes at which these waters are formed.

In the PD simulation, however, the Bering Strait inflow does not lie on the Arctic runoff/NADW mixing line, and therefore changes its gradient. The modelled inflow through the Bering Strait is about twice that observed, so its influence on the northern North Atlantic $\delta^{18}O$:salinity relationship is enhanced. Note that, in the real ocean, if the Bering Strait properties remained the same, changes in the rate of inflow would not affect the Atlantic $\delta^{18}O$:salinity relationship.

Table 1 shows the surface isotope flux for the Atlantic and Arctic, integrated over 10° latitude bands, for the PD experiments. The $\delta^{18}O$-depleted precipitation and runoff at higher latitudes results in a large negative $\delta^{18}O$ forcing to the ocean. In the control experiment, the net isotope flux is − 12.23 ‰ Sv (a positive flux is into the ocean), and the thermohaline circulation exchanges 16 Sv between the Atlantic and Southern Oceans (Fig. 2). For equilibrium, this requires a mean $\delta^{18}O$ difference between the upper inflowing and deep outflowing water of 0.76 ‰. Modelled NADW leaves the South Atlantic with $\delta^{18}O = 0.0$ ‰. Waters with a high $\delta^{18}O$ enter the South Atlantic from the Indian Ocean via the Agulhas Current, with $\delta^{18}O = 0.65$ ‰, whereas water from Drake Passage has a $\delta^{18}O = -0.1$ ‰. This is consistent with a predominantly warm-water return route for the thermohaline circulation, as can be found in the modelled circulation. This contrasts with the study of Juillet-Leclerc et al. (1997), who used an atmospheric GCM with a full isotope model, to derive isotope fluxes between atmosphere and ocean. Their calculated surface isotope fluxes for the Atlantic show a net increased $\delta^{18}O$ flux into the ocean, compared with our results, consistent with lower surface $\delta^{18}O$ values, and

Table 1
Modelled surface fluxes into the Atlantic and Arctic for the PD and LGM

Latitude band (°)	Surface flux (‰ Sv)	
	PD control	LGM control
− 30 → − 20	− 0.35	− 0.58
− 20 → − 10	− 0.57	− 0.96
− 10 → 0	0.40	− 0.19
0 → 10	− 0.45	− 0.54
10 → 20	0.58	− 0.33
20 → 30	0.55	− 0.32
30 → 40	− 0.62	− 1.02
40 → 50	− 1.78	− 1.50
50 → 60	− 2.05	− 2.02
60 → 70	− 1.80	− 1.55
70 → 80	− 3.65	− 3.38
80 → 90	− 2.49	− 2.90
Total Atlantic and Arctic isotope flux	− 12.23	− 15.29

we therefore conclude, an implied cold-water return path (through Drake Passage) for the thermohaline circulation, with low δ^{18}O.

An accurate evaluation of the actual surface isotope flux over the Atlantic would allow the real contributions from the warm and cold-water paths to be determined. The δ^{18}O climatology of Bigg and Rohling (2000) has generally higher surface δ^{18}O over the Atlantic (Fig. 4), which is consistent with a greater δ^{18}O loss from the surface, and therefore, an increased influx of δ^{18}O in the thermohaline return path, which favours the warm-water route. However, the calculation of the δ^{18}O of evaporation (Eq. (2)) is very sensitive to the relative humidity, which was set to 0.75. A lower relative humidity would enhance evaporation and so decrease the surface δ^{18}O flux away from the ocean, resulting in higher surface δ^{18}O values to balance the Atlantic δ^{18}O budget.

In the LGM control experiment, there is a greater surface loss of δ^{18}O than in the PD control experiment (Table 1). This is mainly accounted for in the subtropical regions, where surface temperatures are $\sim 2\,^{\circ}$C cooler than for the PD, but evaporation is little changed due to stronger winds. This decreases the δ^{18}O of evaporation, making the Atlantic and Arctic isotope budget more negative at the LGM.

Decreasing the δ^{18}O of runoff to the Arctic also places the Bering Strait inflow off the Arctic runoff/NADW δ^{18}O:salinity relationship. Such a reduction in the δ^{18}O of Arctic runoff probably occurred at the LGM due to the increased altitude of high-latitude precipitation over the ice sheets. In the LGM simulation, this was found to have a proportional effect on the δ^{18}O:salinity gradient in the northern North Atlantic, because of the absence of Bering Strait inflow. However, in the PD simulation, a depletion in the δ^{18}O of Arctic runoff has to be considered in conjunction with the inflow through the Bering Strait, giving a moderated change in the northern North Atlantic δ^{18}O:salinity gradient. This situation would have occurred during the latter part of the deglaciation, when sea levels had risen sufficiently to allow flow through the Bering Strait (which is 50-m deep at the PD), but there were still inputs of δ^{18}O-depleted glacial meltwater.

The PD control simulation showed a linear relationship between δ^{18}O and salinity from the most depleted to the most enriched δ^{18}O waters, although marginal seas and equatorial regions lie off this line. This suggests that the properties are set by mixing between two end-members, representative of low- and high-latitude fresh water fluxes. This has also been the interpretation of this trend in observational data. However, the sensitivity experiments show that this is a much too simplistic picture. Enhanced depletion of the runoff to the Arctic reveals that the low- to mid-latitude δ^{18}O:salinity relationship is essentially independent of this, and therefore, is set by a balance between the δ^{18}O of the surface fresh water flux, and oceanic advection and mixing within the low- and mid-latitude waters. In the model, mixing with Arctic-origin waters occurs towards the mid-point of this advection/mixing line, causing curvature towards the Arctic water mass properties. The near-horizontal δ^{18}O:salinity line through equatorial and low-latitude North Atlantic points seen in observed data is also present in both the PD and LGM simulations.

The LGM control simulation exhibits a rather different δ^{18}O:salinity relationship. In the absence of Bering Strait inflow, Arctic runoff alone is incorporated into GNADW, as shown by their relationship in δ^{18}O:salinity space. At low- to mid-latitudes, the gradient of the relationship is much reduced. The sensitivity experiment with the δ^{18}O of Arctic runoff at -42‰ is more consistent with the likely δ^{18}O of glacial runoff at the LGM, which should be taken as the most likely scenario for the LGM δ^{18}O:salinity relationship. The surface δ^{18}O for this simulation is shown in Fig. 13. The influence of highly δ^{18}O-depleted Arctic waters extends southward to $\sim 50\,^{\circ}$N in the Atlantic. North of this, the δ^{18}O:salinity gradient is greater than 1.0 (Fig. 10), considerably steeper than at the PD. To the south of this, δ^{18}O values increase by over 1‰ in under 10° of latitude, where the North Atlantic current flows towards Europe. Thus, δ^{18}O should be a good proxy for locating the boundary between polar and sub-tropical origin waters, even if determination of the actual salinity of the water is more problematic.

The dominant influence of oceanic advection in setting up the low- to mid-latitude δ^{18}O:salinity gradient is further demonstrated by the simulations with the oceanic advection of δ^{18}O doubled. The rate of homogenization of water masses by mixing, which is the alternative process for balancing the surface flux

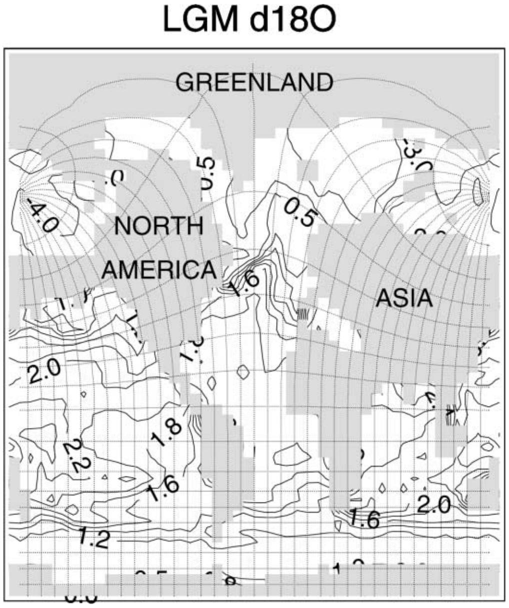

Fig. 13. Last glacial maximum surface $\delta^{18}O$ distribution from the simulation with an Arctic runoff $\delta^{18}O$ of -42 ‰. Note the non-uniform contour interval in these plots.

of $\delta^{18}O$, is unchanged by doubling the advection. The $\delta^{18}O$:salinity gradient of the low- and mid-latitude waters is halved in both the PD and LGM simulations. This is consistent with oceanic advection, not mixing, being the dominant process balancing the surface flux. This, despite the rather strong horizontal mixing coefficients used in coarse resolution models such as this one. Mixing is important during the transport of $\delta^{18}O$-depleted Arctic waters to the North Atlantic, as shown by the unchanged gradient in the mid- to high-latitude $\delta^{18}O$:salinity gradient in the LGM simulation. The corresponding PD simulation is complicated by the additional advection of $\delta^{18}O$ through the Bering Strait.

It has been shown that the $\delta^{18}O$:salinity relationships are sensitive to both ocean advection and the $\delta^{18}O$ of high-latitude inputs. Both of these are known to have changed in the past. This work, therefore, strongly suggests that $\delta^{18}O$:salinity gradients were different at the LGM, but it will require a fully coupled ocean–atmosphere–sea-ice isotope model, run to equilibrium, to gain a more accurate picture of surface $\delta^{18}O$ at the LGM.

8. Conclusions

Modelling of oceanic $\delta^{18}O$ distributions for the PD and LGM, and their sensitivity to Arctic runoff and oceanic advection, has shed new light on the processes controlling oceanic $\delta^{18}O$ distributions in the North Atlantic. The implications for using $\delta^{18}O$ to reconstruct palaeoclimate are considerable, since this work shows that PD $\delta^{18}O$:salinity advection/mixing relationships almost certainly changed in the past, and therefore cannot be used to reconstruct past salinity.

It has been shown that the inflow to the Arctic through the Bering Strait is an important component of the high-latitude North Atlantic $\delta^{18}O$ system. This has not been previously recognised, because the $\delta^{18}O$ and salinity of inflow through the Bering Strait at the PD lie on the mixing line in $\delta^{18}O$:salinity space joining Arctic runoff and NADW. In the early Holocene, when there was still an input of glacial meltwater to the North Atlantic, the increased $\delta^{18}O$-depletion of Arctic runoff would have increased the $\delta^{18}O$:salinity gradient between Arctic runoff and NADW, so that the Bering Strait water would lie on the high salinity side of this line. Increased depletion of the $\delta^{18}O$ of Arctic runoff, due to $\delta^{18}O$-depleted precipitation over high altitude ice sheets, increases the mid- to high-latitude $\delta^{18}O$:salinity gradient. This is independent of the amount of fresh water input, and therefore, changes the PD relationship between $\delta^{18}O$ and salinity, which has been used to reconstruct palaeosalinity.

At low to mid-latitudes in the North Atlantic, the $\delta^{18}O$:salinity gradient is a function of surface fluxes, oceanic advection and mixing, which in the past have been different from those of today. This leads to a much-reduced $\delta^{18}O$:salinity gradient at low to mid-latitudes at the LGM compared with the PD. Finally, the LGM modelled circulation in the North Atlantic has a much reduced exchange with the rest of the global ocean than in the PD circulation. This increased recirculation within the Atlantic complicates the surface balance resulting from the surface flux of $\delta^{18}O$, making climatic inferences from records of past surface $\delta^{18}O$ all the more elusive.

The modelling work presented here advances the theoretical arguments of Rohling and Bigg (1998), and confirms their assertion that oceanic advection plays a crucial role in determining oceanic $\delta^{18}O$ distributions. It also confirms the finding of Schmidt (1998) that the δ^{18}O:salinity relationship changes with changes in ocean circulation. Forward modelling of proxy δ^{18}O data in climate models, and validation through comparisons with real proxy data, now probably offers the most appropriate way of improving our knowledge of past climates.

Acknowledgements

We would like to thank the Leverhulme Trust for supporting this work under Grant F204Q.

References

Baertschi, P., 1976. Absolute ^{18}O of standard mean ocean waters. Earth Planet. Sci. 31, 341–344.

Bauch, D., Schlosser, P., Fairbanks, R.G., 1995. Freshwater balance and the sources of deep and bottom waters in the Arctic Ocean inferred from the distribution of $H_2{}^{18}O$. Prog. Oceanogr. 35, 53–80.

Beare, M.H., 1998. The Southampton–East Anglia parallel ocean circulation model: equations and finite difference scheme. (http://www.mth.uea.ac.uk/ocean/SEA).

Bigg, G.R., Rohling, E.J., 2000. An oxygen isotope data set for marine waters. J. Geophys. Res. 105 (C4), 8527–8536.

Bigg, G.R., Wadley, M.R., 2001. The origin and flux of icebergs released into the Last Glacial Maximum northern hemisphere oceans: the impact of ice sheet topography. J. Quaternary Science (in press).

Boyle, E., 1995. Last glacial maximum North Atlantic deep water—on, off or somewhere in between. Philos. Trans. R. Soc. London, Ser. B 348, 243–253.

Bryan, K., 1969. A numerical method for studying the circulation of the world ocean. J. Comput. Phys. 4, 347–376.

Bryan, K., 1984. Accelerating the convergence to equilibrium of ocean-climate models. J. Phys. Oceanogr. 14, 666–673.

CLIMAP, 1981. Climate. Long-range investigation, mapping and prediction (CLIMAP) project members, seasonal reconstruction of the earth's surface at the last glacial maximum. Geol. Soc. Am., Map Chart Ser., MC-36.

Coachman, L.K., Aagaard, K., 1988. Transports through Bering Strait — annual and interannual variability. J. Geophys. Res. 93 (C12), 15535–15539.

Cox, M.D., 1984. A primitive equation three-dimensional model of the ocean. Technical Report 1, GFDL Ocean Group, Geophysical Fluid Dynamics Laboratory/NOAA, Princeton, NJ.

Dong, B., Valdes, P.J., 1998. Simulations of the Last Glacial Maximum climates using a general circulation model: prescribed versus computed sea surface temperatures. Clim. Dym. 14, 571–591.

Duplessy, J.C., Bard, E., Labeyrie, L., Duprat, J., Moyes, J., 1993. Oxygen isotope records and salinity changes in the northeastern Atlantic Ocean during the last 18,000 years. Paleoceanogr. 8, 341–350.

England, M.H., 1993. Representing the global-scale water masses in ocean general circulation models. J. Phys. Oceanogr. 23, 1523–1552.

ETOPO, 1986. Global $5' \times 5'$ depth and elevation. (Available from National Geophysical Data Centre, NOAA, US Dept. Of Commerce, Code E/GC3, Boulder, CO 80303).

Fairbanks, R.G., 1989. A 17,000 year glacio-eustatic sea level record — influence of glacial meltwater rates on the Younger Dryas event and deep-ocean circulation. Nature 342, 637–642.

Fairbanks, R.G., Matthews, R.K., 1978. The marine oxygen isotope record in Pleistocene coral, Barbados, West Indies. Quat. Res. 10, 181–196.

Ferronsky, V.I., Brezgunov, V.S., 1982. Stable isotopes and ocean dynamics. In: Ferronsky, V.I., Polyakov, V.A. (Eds.), Environmental Isotopes in the Hydrosphere. Wiley, Chichester, England, pp. 1–27.

Frew, R.D., Heywood, K.J., Dennis, P.F., 1995. Oxygen isotope study of water masses in the Princess Elizabeth Trough, Antarctica. Mar. Chem. 49, 141–153.

Frew, R.D., Dennis, P.F., Heywood, K.J., Meredith, M.P., Boswell, S.M., 2000. The oxygen isotope composition of water masses in the northern North Atlantic. Deep-Sea Res. 47, 2265–2286.

Ganopolski, A., Rahmstorf, S., Petoukhov, V., Claussen, M., 1998. Simulation of modern and glacial climates with a coupled global model of intermediate complexity. Nature 391, 350–356.

Gat, J.R., 1996. Oxygen and hydrogen isotopes in the hydrologic cycle. Annu. Rev. Earth Planet. Sci. 24, 225–262.

Gat, J.R., Gonfiantini, R. (Eds.), 1981. Stable Isotope Hydrology: Deuterium and Oxygen-18 in the Water Cycle. International Atomic Energy Agency, Vienna, 340 pp.

Gat, J.R., Shemesh, A., Tziperman, E., Hecht, A., Georgopoulos, D., Basturk, O., 1996. The stable isotope composition of waters of the eastern Mediterranean Sea. J. Geophys. Res. 101 (C3), 6441–6451.

Gordon, A.L., 1986. Inter-ocean exchange of thermocline water. J. Geophys. Res. 91 (C4), 5037–5046.

Gorshkov, S.G. (Ed.), 1978. World Ocean Atlas. Atlantic and Indian Oceans, vol. 2, Pergamon, Tarrytown, NY, 306 pp.

Griffies, S.M., Gnanadesikan, A., Pacanowski, R.C., Larichev, V., Dukowicz, J.K., Smith, R.D., 1998. Isoneutral diffusion in a *z*-coordinate ocean model. J. Phys. Oceanogr. 28, 831–841.

Hebbeln, D., Dokken, T., Andersen, E.S., Hald, M., Elverhoi, A., 1994. Moisture supply for northern ice-sheet growth during the Last Glacial Maximum. Nature 370, 357–360.

Hellerman, S., Rosenstein, M., 1983. Normal monthly wind stress over the world's ocean with error estimates. J. Phys. Oceanogr. 13, 1093–1104.

Joussaume, S., Jouzel, J., 1993. Paleoclimate tracers — an investigation using an atmospheric general circulation model under ice-age conditions: 2. Water isotopes. J. Geophys. Res. 98 (D2), 2807–2830.

Juillet-Leclerc, A., Jouzel, J., Labeyrie, L., Joussaume, S., 1997. Modern and last glacial maximum sea surface δ^{18}O derived from an atmospheric general circulation model. Earth Planet. Sci. Lett. 146, 591–605.

Labeyrie, L.D., Duplessy, J.C., Blanc, P.L., 1987. Variations in the mode of formation and temperature of oceanic deep waters over the past 125,000 years. Nature 327, 477–482.

Labeyrie, L.D., Duplessy, J.C., Duprat, J., Juillet-Leclerc, A., Moyes, J., Michel, E., Kallel, N., Shackleton, N.J., 1992. Changes in the vertical structure of the North Atlantic Ocean between glacial and modern times. Quat. Sci. Rev. 11, 401–413.

Levitus, S., Boyer, T.P., 1994. World Ocean Atlas 1994. Salinity, vol. 3, NOAA NESDIS Atlas, Washington, DC.

Levitus, S., Burgett, R., Boyer, T.P., 1994. World Ocean Atlas 1994. Temperature, vol. 4, NOAA NESDIS Atlas, Washington DC.

Nowlin, W.D., Klinck, J.M., 1986. The physics of the Antarctic circumpolar current. Rev. Geophys. 23 (4), 459–491.

Oberhuber, J.M., 1988. An atlas based on the 'COADS' data set: the budgets of heat, buoyancy and turbulent kinetic energy at the surface of the global ocean. Max-Planck-Institut fuer Meteorologie (Hamburg) Rep. 15, 199 pp.

Östlund, H.G., Hut, G., 1984. Arctic Ocean water mass balance from isotope data. J. Geophys. Res. 89 (C4), 6373–6381.

Rohling, E.J., Bigg, G.R., 1998. Paleosalinity and $\delta^{18}O$: a critical assessment. J. Geophys. Res. 103, 1307–1318.

Sarnthein, M., Jansen, E., Weinelt, M., Arnold, M., Duplessy, J.C., Erlenkeuser, H., Flatoy, A., Johannessen, G., Johannessen, T., Jung, S., Koc, N., Labeyrie, L., Maslin, M., Pflaumann, U., Schulz, H., 1995. Variations in Atlantic surface ocean paleoceanography, 50° to 80° N — A time-slice record of the last 30,000 years. Paleoceanogr. 10, 1063–1094.

Schmidt, G.A., 1998. Oxygen-18 variations in a global ocean model. Geophys. Res. Lett. 25, 1201–1204.

Schmidt, G.A., 1999. Forward modeling of carbonate proxy data from planktonic foraminifera using oxygen isotope tracers in a global ocean model. Paleoceanogr. 14, 482–497.

Schmitz, W.J., 1995. On the interbasin-scale thermohaline circulation. Rev. Geophys. 33, 151–173.

Semtner, A.J., 1974. A general circulation model for the world ocean, Technical Report 8, Department of Meteorology, University of California, Los Angeles.

Shackleton, N.J., 1987. Oxygen isotopes, ice volume and sea level. Quat. Sci. Rev. 6, 183–190.

Speer, K.G., Zenk, W., 1993. The flow of Antarctic bottom water into the Brazil Basin. J. Phys. Oceanogr. 23, 2667–2682.

Thompson, S.R., 1995. Sills of the global ocean: a compilation. Ocean Modell. 109, 7–9.

Veum, T., Jansen, E., Arnold, M., Beyer, I., Duplessy, J.C., 1992. Water mass exchange between the North Atlantic and Norwegian Sea during the last 28,000 years. Nature 356, 783–785.

Wadley, M.R., Bigg, G.R., 2000. Implementation of variable time stepping in an ocean general circulation model. Ocean Modell. 1, 71–80.

Wadley, M.R., Bigg, G.R., 2001. Impact of flow through the Canadian Archipelago on the North Atlantic and Arctic thermohaline circulation: an ocean modelling study. Q. J. R. Meteorol. Soc. (Submitted for publication).

Wang, L., Sarnthein, M., Duplessy, J.C., Erlenkeuser, H., Jung, S., Pflaumann, U., 1995. Paleo sea-surface salinities in the low-latitude Atlantic. The $\delta^{18}O$ record of Globigerinoides ruber (white). Paleoceanogr. 10, 749–761.

Zreda, M., England, J., Phillips, F., Elmore, D., Sharma, P., 1999. Unblocking of Nares Strait by Greenland and Ellesmere ice-sheet retreat 10,000 years ago. Nature 398, 139–142.